2021 IEEE Computer Society Annual Symposium on VLSI (ISVLSI) | 978-1-6654-3946-6/21/$31.00 ©2021 IEEE | DOI: 10.1109/ISVLSI51109.2021.00066

Oscillatory Neural Networks for Edge AI Computing

Corentin Delacour
Microelectronics Department
LIRMM, Univ. of Montpellier, CNRS
Montpellier, France
Email: corentin.delacour@lirmm.fr

Stefania Carapezzi
Microelectronics Department
LIRMM, Univ. of Montpellier, CNRS
Montpellier, France
ORCID: 0000-0002-9271-1189

Madeleine Abernot
Microelectronics Department
LIRMM, Univ. of Montpellier, CNRS
Montpellier, France
Email: madeleine.abernot@lirmm.fr

Gabriele Boschetto
Microelectronics Department
LIRMM, Univ. of Montpellier, CNRS
Montpellier, France
ORCID: 0000-0001-8830-3572

Nadine Azemard
Microelectronics Department
LIRMM, Univ. of Montpellier, CNRS
Montpellier, France
Email: nadine.azemard@lirmm.fr

Jeremie Salles
Microelectronics Department
LIRMM, Univ. of Montpellier, CNRS
Montpellier, France
Email: jeremie.salles@lirmm.fr

Thierry Gil
Microelectronics Department
LIRMM, Univ. of Montpellier, CNRS
Montpellier, France
Email: thierry.gil@lirmm.fr

Aida Todri-Sanial
Microelectronics Department
LIRMM, Univ. of Montpellier, CNRS
Montpellier, France
ORCID: 0000-0001-8573-2910

***Abstract*—In this paper, we showcase the innovative concept of implementing Oscillatory Neural Networks (ONNs) for neuromorphic computing with beyond-CMOS devices based on vanadium dioxide to mimic neurons and resistors to emulate synapses. We explore ONN technology potentials from device to analog circuit-level simulations. We report that ONN behaves like an associative memory and can implement energy-based models such as Hopfield Neural Networks on edge devices. Finally, as a proof of concept, a reconfigurable digital ONN is implemented on FPGA for pattern recognition tasks.**

***Index Terms*—Oscillatory neural networks (ONN), Internet-of-Things (IoT), Edge Artificial Intelligence (edge AI), Neuromorphic Computing, Beyond-CMOS devices, Technology Computer-Aided Design (TCAD), FPGA**

I. Introduction

Classical computing based on the von Neumann paradigm suffers from the communication bottleneck between memory and processor, which causes a significant limitation for data processing. To keep up with the ever-increasing data growth from connected IoT devices and intelligent agents [1], referred to as "data deluge," there are tremendous efforts to develop a novel computing paradigm inspired by brain-like computing to process the data where data is available meaning at the edge devices. This has resulted in industry and academic communities investigating in-memory computing by exploring novel material, devices, circuits, and architecture design styles to enable massive parallelism and energy-efficient computing [2].

Over the last decades, computing with artificial neural networks (ANNs) and convolutional neural networks (CNNs) have revolutionized Artificial Intelligence (AI) in every aspect of society from healthcare, autonomous driving, entertainment, among others. Yet, these powerful neural networks run on classical systems such as CPUs, GPUs, or TPUs, which suffer from energy inefficiency and deployment at the edge [3]. Alternatively, a new class of artificial neural networks based on coupled oscillators or Oscillatory Neural Networks (ONN) draws a lot of interest as a low power computing paradigm that can enable online learning and inference at the edge [4]. ONN is based on analog computing, where information is encoded on the phase relations between oscillators with the key concept of "let physics compute" [5], [6].

The novelty in ONNs is to harness the rich dynamics of coupled oscillators to compute in the phase domain rather than amplitude domain as in other artificial or spiking neural networks. This means that the signal amplitude can be extremely low, resulting in a low power computing solution [7]. Oscillators physically emulate neuronal oscillatory behavior (e.g., brain waves), and resistors emulate synaptic coupling between neurons. Such architecture enables in-memory computing where both processing (oscillators) and memory (synapses) constitute a truly parallel analog computing architecture.

ONN computational capacity has been studied and proved by mathematicians for decades [5], but hardware implementations were limited. The emergence of energy-efficient and

This work was supported by the European Union's Horizon 2020 research and innovation programme, EU H2020 NEURONN (www.neuronn.eu) project under Grant 871501.

978-1-6654-3946-6/21/$31.00 ©2021 IEEE
DOI 10.1109/ISVLSI51109.2021.00066

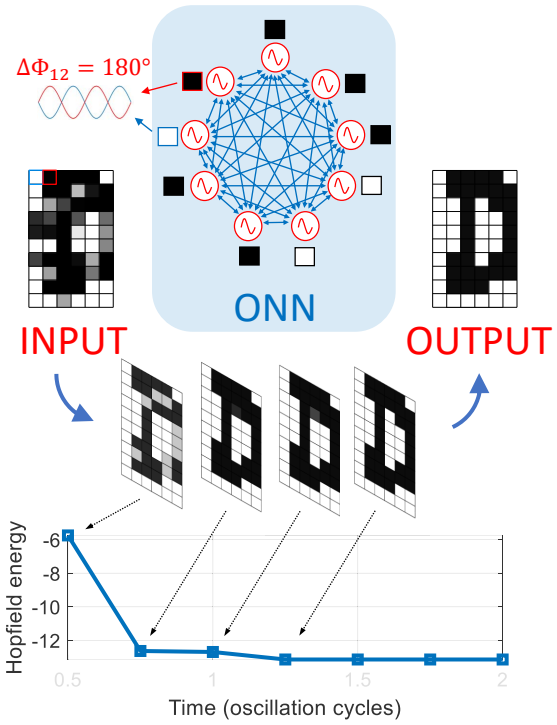

Fig. 1. ONN as associative memory, like a Hopfield Neural Network (60 oscillators in this example). Every oscillator is coupled to all others via resistors. Gray-scale images represent the ONN phase state. ONN stores pattern 'D,' which can be retrieved from noisy input patterns. ONN phase state evolves such that the conceptual Hopfield energy [5] reaches a minimum corresponding to a stored pattern.

compact oscillators based on vanadium dioxide (VO_2) incites a new interest in ONN implementation. Up to 6 VO_2-oscillators have been coupled experimentally [7], and it is expected that this number will increase with the progress on device fabrication.

In this work, we perform device to circuit-level ONN simulations based on VO_2-oscillators. We have developed a design tool flow to allow material properties, device to circuit-level modeling for exploring the potential of ONN computing. We report on performances and energy-efficiency up to 60 coupled VO_2-oscillators for pattern recognition, like a Hopfield Neural Network (HNN) [8]. Finally, as a proof-of-concept, we developed a digital ONN architecture and implemented it in an FPGA for testing AI workloads.

II. ONN Computing Paradigm

A. Phase-based computing

A large number of physical phenomena can be modeled in terms of interacting oscillator dynamics. In biology, cellular processes such as the glycolytic system of muscle cells have oscillatory behavior [9]. From neuroscience, there is evidence that biological oscillators are synchronized through coupling via signaling messengers like hormones [9]. Also, neurons can sometimes be represented as oscillators [10] and recent brain

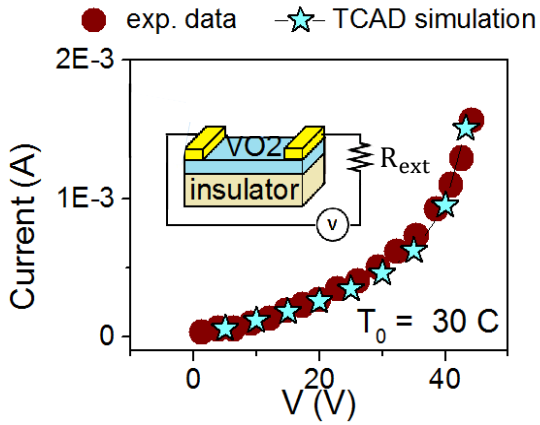

Fig. 2. Experimental and simulated I-V curves (up to IMT switching) of VO_2 device (thickness 200 nm, width 100 μm and length 5 μm) [22]. R_{ext} is a 5 kΩ external resistor.

studies [11] have demonstrated that signals from a sensory cortex can affect activity in another one by synchronizing neural oscillations. This suggests that phase-based computing possesses benefits that can be biomimetically exploited in hardware, such as ONNs.

In ONNs, information is encoded in the phase between oscillators, and the first oscillator is used as reference [12]. ONN input is the initial ONN phase state, which evolves until it settles to a stable fixed point. ONN output is given by the final oscillator phases that take binary values $\Delta\Phi^{out} \epsilon \{0°; 180°\}$. ONN phase state evolution can be interpreted as the minimization of an energy function in the phase space [5], as in HNNs. Conceptually, ONN inference consists of exploring the energy landscape to reach the minima that correspond to stable phase states. ONN's initial state corresponds to an initial point in energy space that reaches a local minimum after a settling time.

B. ONN as an associative memory

ONN behaves like an associative memory when oscillators are fully connected, i.e., every oscillator is connected to all others via resistors. In this case, ONN training consists of storing patterns that can be retrieved with partial input information (like a noisy input) [5]. Conveniently, binary phase states $\Delta\Phi = 180°$ and $\Delta\Phi = 0°$ can be represented as black and white pixels of an image, respectively (a pixel corresponds to a single oscillator). In this work, we explore pattern recognition application by simulating coupled VO_2-oscillators as an associative memory (Fig.1).

III. ONN Devices to Circuits

A. VO_2 device

Vanadium dioxide (VO_2) is a transition metal oxide that undergoes a phase change at 340 K, close to room temperature: it switches from an insulating monoclinic M_1 phase to a

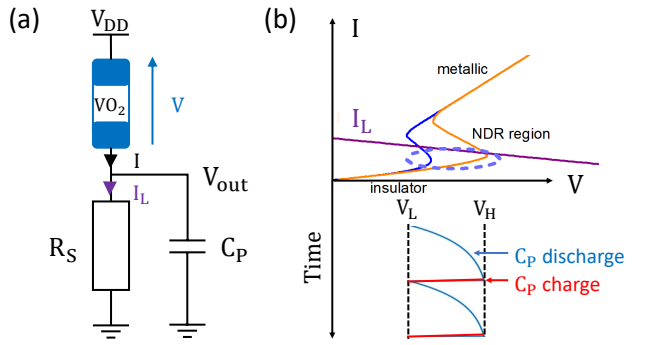

Fig. 3. a) VO_2-oscillator circuit. b) Example of VO_2 $I-V$ curve and evolution of the device voltage. VO_2 hysteresis behavior is used to produce oscillations by biasing the VO_2 device in its Negative Differential Region (NDR).

metallic rutile R phase, with a sharp change in resistivity up to 5 orders of magnitude. Such insulator-to-metal transition (IMT) is reversible, making VO_2 suitable for switches and memory devices. The mechanism of the IMT is not yet fully understood. However, it is now believed that a strong electron-electron correlation and an electron-phonon interaction both play an important role: this suggests a Mott-Peierls transition mechanism [13]. Moreover, the properties of the phase transition of VO_2 can be tuned, for instance, by doping with metal atoms, by introducing defects, and by induced stress at the interface of grain boundaries [14].

Experimental results indicate that self-heating initiates the IMT of VO_2 in biased devices [15]. Electrothermal simulations at the device level assist in 1) understanding the underlying device physics and 2) switching mechanism. We have developed a dedicated technology computer-aided design (TCAD) procedure to simulate VO_2 devices. We use doping density to mimic the temperature-dependent change of resistivity inside the VO_2 channel. The match between experimental and simulated data provides a good fit (Fig. 2), confirming that self-heating prompts IMT transition.

In ONN circuits, IMT and metal-to-insulator transitions (MIT) of VO_2 devices are exploited to design relaxation oscillators [18]. When VO_2 device's voltage V is above a threshold V_H, its current flow induces IMT switching, and the device stays in the metallic state as long as V remains larger than a lower threshold V_L. When $V < V_L$, VO_2 transitions to an insulating state (MIT). Thus, VO_2 has a hysteresis in its $I-V$ curve (Fig.3b) that is used in oscillatory circuits.

To embed the VO_2 device description into circuit-level simulations, we developed a tool flow TCAD-SPICE, where the role of TCAD is to assist compact modeling for circuit simulations. Specifically, VO_2 metallic and insulating resistances, associated with both voltage thresholds, serve as input to a SPICE VO_2 model [16].

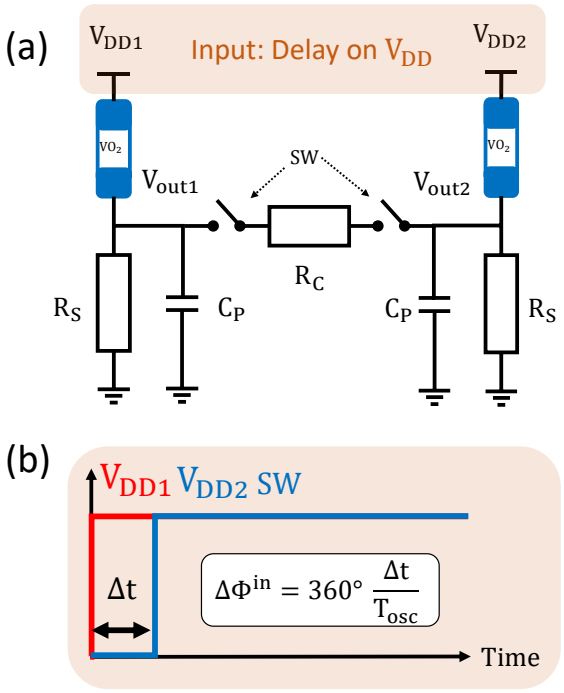

Fig. 4. a) Two identical VO_2-oscillators coupled by a resistor R_C that can be disconnected via switches. b) The starting-time of the second oscillator is delayed via V_{DD2} to set an initial phase, and the switches are closed to compute.

B. VO_2-oscillator

Similar to Schmitt-trigger based oscillators, we use VO_2 hysteresis behavior to design compact relaxation oscillators. We bias the VO_2 device with a resistor R_S in series (Fig.3a). To obtain oscillations, the load line I_L intercepts VO_2 $I-V$ characteristic in its Negative Differential Region (NDR). In this case, the output capacitor C_P charges through the VO_2 device in the metallic state and discharges through R_S when the VO_2 device is in an insulating state. V_L and V_H VO_2 threshold voltages define the oscillation amplitude. For a given VO_2 device, R_S and C_P set the oscillation frequency (in this work R_S=20 kΩ and C_P=500 pF gives f=46.3 kHz). The oscillating output signal is the voltage across C_P, and the input is the supply voltage starting time. To set an initial input phase between two oscillators, we delay the starting time of the second oscillator's supply voltage with respect to the first oscillator.

C. Two coupled-oscillators circuit

Fig.4a shows the smallest ONN consisting of two oscillators coupled by a resistor R_C. We insert switches in series with R_C to decouple oscillators during initialization [17]. To set an input phase state $\Delta\Phi^{in}$ between two oscillators, we delay the second oscillator's supply voltage starting time, as shown in Fig.4b. Once all oscillators are turned on, we close the switches to couple the oscillators.

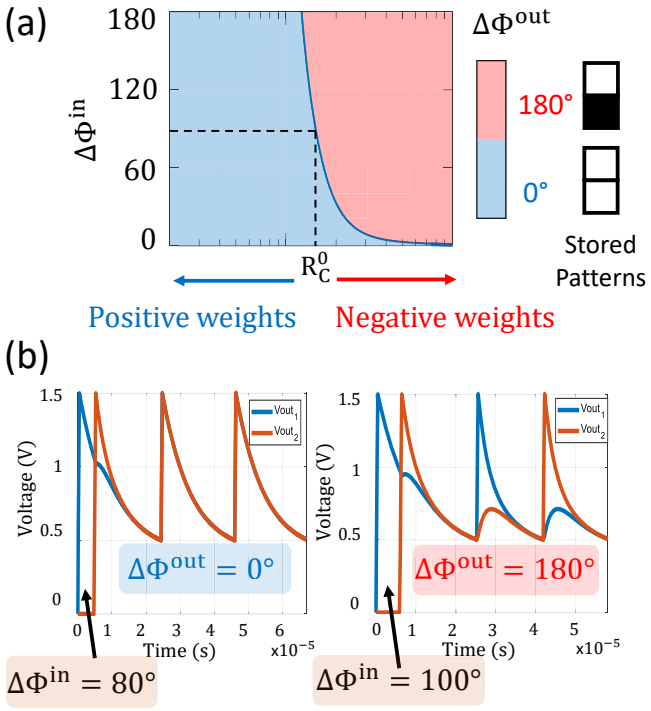

Fig. 5. a) $\Delta\Phi^{out}$ extracted after convergence for every set of parameters $(R_C, \Delta\Phi^{in})$. Positive weights are mapped to small coupling resistances, whereas negative weights are implemented with large R_C. At $R_C = R_C^0$, two distinct states are memorized, corresponding to the right-hand side patterns. b) Output voltages of the two oscillators for $R_C = R_C^0$. Left: $\Delta\Phi^{in} = 80°$ and the oscillators converge to a stable in-phase state. Right: $\Delta\Phi^{in} = 100°$ and the oscillators converge to a stable out-of-phase state.

After a few cycles, both oscillators settle to a stable phase state, and we can measure their phase difference. Both $\Delta\Phi^{in}$ and R_C influence the final phase state outcome $\Delta\Phi^{out}$. Fig.5a shows $\Delta\Phi^{out}$ obtained for various R_C and inputs $\Delta\Phi^{in}$. We observe that a small $R_C << R_C^0$ induces $\Delta\Phi^{out} = 0°$, whereas a large $R_C >> R_C^0$ leads to $\Delta\Phi^{out} = 180°$, as already noticed in [18]. These phase states can be represented by two distinct patterns stored in ONN via R_C values. Particularly, for $R_C = R_C^0$, we equally retrieve both patterns by adjusting $\Delta\Phi^{in}$ (Fig.5b). In other words, two coupled oscillators behave like an associative memory, where R_C contains the memory, and $\Delta\Phi^{in}$ is the input to recall a stored pattern. In the next section, we demonstrate this concept to 60 coupled oscillators using the same initialization procedure and scaling coupling resistances.

IV. ONN Pattern Recognition

To showcase the associative properties of a larger VO_2-ONN architecture, we perform circuit-level simulations of 60 fully-coupled VO_2-oscillators. There are 60x59/2=1770 different synapses, all modeled by ideal resistors that values are determined during the ONN training [17]. In hardware, synapses could be implemented by a resistive cross-bar array with programmable resistors or memristors [2].

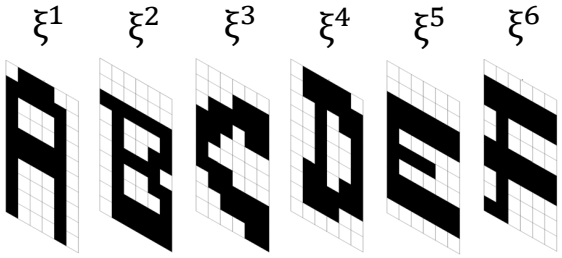

Fig. 6. Six training patterns ξ^k with 60 black and white pixels used in this example. $\xi_i^k = 1$ if pixel i is white and $\xi_i^k = -1$ otherwise. Synaptic weights are computed using the Hebbian rule [5] and are then mapped to coupling resistances to perform circuit simulations.

A. Training and Inference

We study a simple pattern recognition application where six patterns ξ^k are stored in ONN representing letters 'A' to 'F' (Fig.6). To train the ONN, we use the Hebbian rule [5], which gives synaptic coefficients based on ξ^k. We map Hebbian coefficients to coupling resistances, as described in section 3 (Fig.5a).

The recognition operation consists of associating an input pattern to one of the training patterns. A black pixel i corresponds to $\Delta\Phi_i^{in} = 180°$ that is set by delaying V_{DDi} by $T_{osc}/2$. A white pixel corresponds to an oscillator in phase with the reference oscillator, thus without any delay. Gray pixels are initialized by delaying oscillators between 0 and $T_{osc}/2$. When the input is sufficiently close to one of the training patterns, ONN retrieves it after a few oscillation cycles. Sometimes, ONN converges toward spurious patterns when the input is too noisy (Fig.7a). In that case, ONN cannot be considered as accurate.

B. ONN performances

We add random noise to training patterns to generate a test set, where noisy pixels take values between -1 and +1. We vary the amount of noise from 0 to 50% of the number of pixels, and we report on ONN recognition accuracy as in Fig.7b. Pattern recognition is unacceptable if a single output pixel differs from the original training pattern. If we tolerate two wrong output pixels, the recognition accuracy increases, meaning that ONN sometimes locks to spurious patterns that are close to the training patterns. Evaluating ONN accuracy with the test set, we observe that ONN has more than 60% of accuracy for test images with up to 30% of noise.

During the test set evaluation, we report an average settling time of 3.9 oscillation cycles (i.e., the required time for the ONN to reach a stable phase state), in accordance with the 4-5 cycles observed in experiments [19]. ONN operates fast thanks to coupled oscillators that work in parallel. We compute the average energy associated with ONN inference and report it on Table I. We notice that the total energy consumption for 60 VO_2-oscillators is $E_{60} \approx 3.9 \times 60 \times E_{/cycle}$, with $E_{/cycle}$ the energy consumed by a single oscillator during one cycle. Hence, we expect a linear energy scaling for larger ONNs.

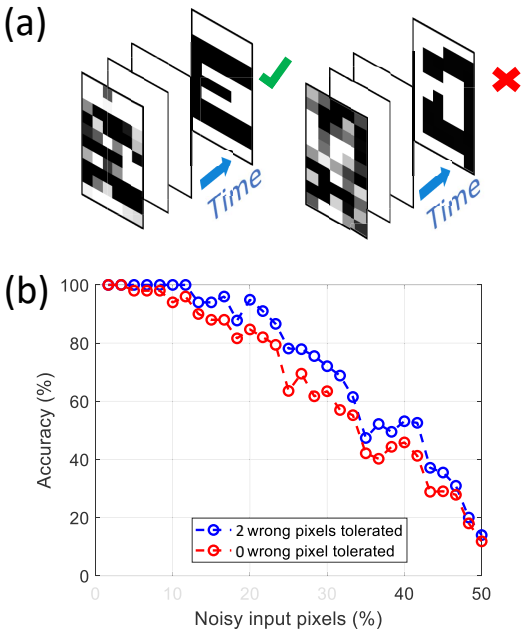

Fig. 7. a) Left: pattern 'E' with 20 randomly altered pixels is applied to the ONN and successfully identified after a few oscillations. Right: pattern 'D' with 28 randomly altered pixels is not identified as the ONN converges to an unknown phase state. b) ONN recognition accuracy with respect to the number of noisy input pixels. For each configuration, 100 simulations are performed using random test patterns. Performances decrease significantly for more than 30 % of input fuzzy pixels.

Based on this observation, we compute the ONN energy for 28x28=784 oscillators required to perform pattern recognition on the MNIST dataset.

In this work, we simulate "slow" oscillators (f=46.3 kHz) to reproduce experiments that were conducted with a large load capacitance C_P=500 pF and high supply voltage V_{DD}=2.5V. However, if VO_2 devices are scaled down with smaller load capacitances and lower supply voltage, we expect a reduced energy footprint [19]. Thus, we apply our ONN energy estimation for scaled VO_2 devices reported in literature [7], [19].

Moreover, we compare our ONN energy prediction with an example of a state-of-the-art edge processor [25], which implements an HNN for pattern recognition. In HNN [8], at least N(N-1) MAC (multiple-accumulate) operations are required to compute the HNN state. We estimate the processor energy consumption as N(N-1)E_{MAC} and assuming 1 MAC $\approx$ 2 OP. Our ONN energy estimation is optimistic as we do not consider all the peripheral circuits to initialize and read-out ONN. Nevertheless, the trend shows that ONN can be a very competitive architecture for less than 800 neurons, as ONN with scaled VO_2 devices [19] would allow a 4000x energy reduction compared to state-of-the-art edge processor [25].

C. ONN on FPGA

We implement a digital ONN-on-FPGA to quantitatively assess the performance metrics of ONN architectures in real-world applications. Our ONN-on-FPGA is inspired by a hybrid analog-digital solution [26], but we have implemented a fully digital architecture [27]. Digital neurons oscillate at 488 kHz.

TABLE I
ONN ENERGY FOOTPRINT

	This work	ONN [7]	Scaled ONN prediction [19]	Coral Edge TPU [25]
$E_{/cycle}$ or E_{MAC}	2.15 nJ	120 pJ	50 fJ	1 pJ
E_{60}	494 nJ	28 nJ	11.7 pJ	3.5 nJ
E_{784}	6.6 μJ	367 nJ	153 pJ	614 nJ

We use pattern recognition as a testbed as it is a typical edge AI task. For instance, one could embed low-power ONNs into edge camera systems for image post-processing, noise filtering, or object detection at the interface with sensors. Here, we perform image recognition with a 60-neurons ONN-on-FPGA using the same training set previously defined (Fig.6).

ONN synaptic weights are computed offline via Matlab using the Hebbian learning rule [5]. Weights are subsequently hardcoded inside the FPGA. Fig. 8 describes the experimental procedure that has been set up. Images are streamed by a cell phone and captured by a camera. Then images are re-scaled to 60 pixels to fit the ONN size and used as input to the ONN-on-FPGA. Finally, the output image is re-scaled to be displayed on an HDMI screen once synchronization is achieved.

We evaluate ONN-on-FPGA performances on a test set composed of 30 corrupted training patterns. Only 6 test patterns could not be retrieved correctly (80% recognition accuracy). We measured the time required from ONN initialization to the end of the computation. It has resulted in an average of 13μs (7.8μs initialization and 5.2 μs settling time), demonstrating the real-time computation capability of our ONN-on-FPGA.

V. Conclusions

In this work, we presented an innovative concept for neuromorphic computing based on oscillatory neural networks implemented with beyond-CMOS devices such as vanadium dioxide (VO_2) to emulate neurons and resistors to implement synapses. We explored the ONN technology from devices, circuits to architecture-level implementation. To do so, we developed a dedicated TCAD procedure for VO_2 device simulation to capture its resistive switching mechanism in circuit simulations. Then, we investigated the dynamics of two VO_2-oscillators coupled by a resistor, showing that they naturally behave like an associative memory. We also assessed the performances of larger ONNs and showed that ONN is a competitive paradigm for edge applications thanks to their energy efficiency. Finally, we reported on an ONN-on-FPGA as a proof-of-concept for real-world pattern recognition applications.

As future directions for our work, we aim to complete the entire simulation toolchain from Density Functional Theory (DFT) to TCAD to circuit simulation by designing customized compact models. This will provide precise assessments of

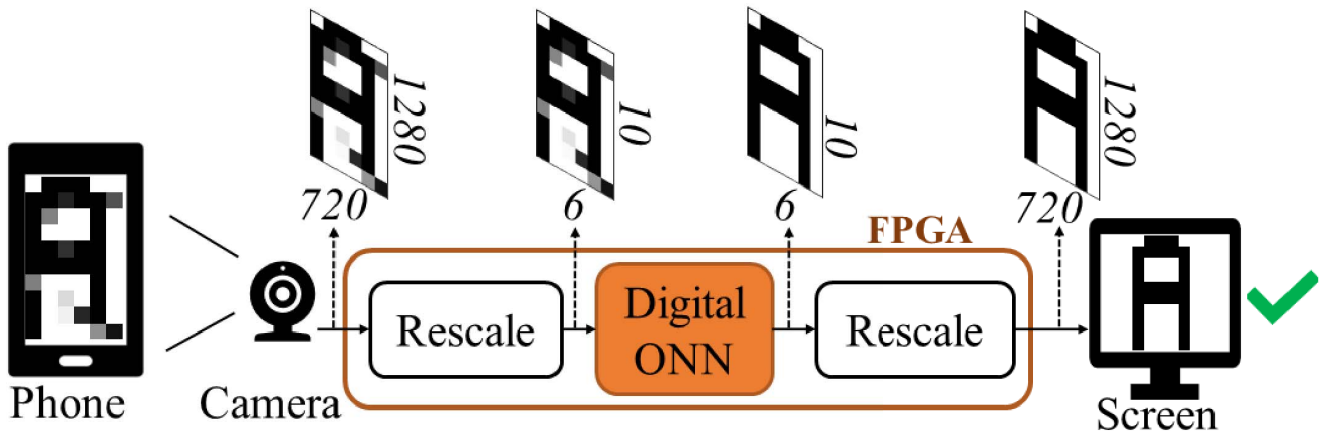

Fig. 8. Workflow of image recognition procedure by digital ONN-on-FPGA; close to each image are indicated the pixel sizes.

ONN power, performance, area, and reliability. Finally, we are exploring the real-time capability of ONN-on-FPGA for other edge AI applications such as autonomous motion-control systems for robotics.

REFERENCES

[1] M. Merenda, C. Porcaro, and D. Iero, "Edge machine learning for AI-enabled IoT devices: a review," Sensors, vol. 20, no. 9, 2533, 2020.

[2] J. D. Kendall and S. Kumar, "The building blocks of a brain-inspired computer," Appl. Phys. Rev., vol. 7, no. 1, 2020.

[3] T. Yang, Y. Chen, J. Emer and V. Sze, "A method to estimate the energy consumption of deep neural networks," 2017 51st Asilomar Conference on Signals, Systems, and Computers, Pacific Grove, CA, U.S.A., 2017.

[4] G. Csaba, and W. Porod, "Coupled oscillators for computing: a review and perspective," Appl. Phys. Rev., vol. 7, 011302, 2020.

[5] F.C. Hoppensteadt, and E.M. Izhikevich, "Pattern recognition via synchronization in phase-locked loop neural networks," IEEE Trans. Neural Netw., vol. 11, pp. 734–738, 2000.

[6] A. Raychowdhury, A. Parihar, G. H. Smith, V. Narayanan, G. Csaba, M. Jerry, et al., "Computing with networks of oscillatory dynamical systems," Proc. IEEE, vol. 107, pp. 73–89, 2019.

[7] N. Shukla, W. -. Tsai, M. Jerry, M. Barth, V. Narayanan and S. Datta, "Ultra low power coupled oscillator arrays for computer vision applications," 2016 IEEE Symposium on VLSI Technology, Honolulu, HI, U.S.A., pp. 1-2 2016.

[8] J.J. Hopfield, "Neural networks and physical systems with emergent collective computational abilities," Proc. Natl. Acad. Sci. U.S.A., vol. 79, pp. 2554–2558, 1982.

[9] J.-R. Kim, D. Shin, S. H. Jung, P. Heslop-Harrison, H.-H. Cho, "A design principle underlying the synchronization of oscillations in cellular systems", J. Cell Sci., vol. 123, pp. 537–543, 2010.

[10] K. M. Stiefel, and G. B. Ermentrout, "Neurons as oscillators," J. Neurophysiol., vol. 116, no. 6, pp. 2950–2960, 2016.

[11] A.-K. R. Bauer, S. Debener, and A. C. Nobre, "Synchronisation of neural oscillations and cross-modal influences", Trends Cogn. Sci., vol. 24, pp. 481–495, 2020.

[12] A. Todri-Sanial, S. Carapezzi, C. Delacour, M. Abernot, T. Gil, E. Corti, S. Karg, J. Martinez Manuel Jiménez, M. Avedillo and B. Linares-Barranco, "How Frequency Injection Locking Can Train Oscillatory Neural Networks to Compute in Phase," working paper or preprint, https://hal-lirmm.ccsd.cnrs.fr/lirmm-03164135, 2021.

[13] T. L. Cocker, L. V. Titova, S. Fourmaux, G. Holloway, H.-C. Bandulet, D. Brassard, et al., "Phase diagram of the ultrafast photoinduced insulator-metal transition in vanadium dioxide," Phys. Rev. B, vol. 85, 155120, April 2012.

[14] S. Chen, J. Liu, L. Wang, H. Luo, Y. Gao, "Unraveling mechanism on reducing thermal hysteresis width of VO_2 by Ti doping: a joint experimental and theoretical study," J. Phys. Chem. C, vol. 118, pp. 18938–18944, August 2014.

[15] A. Zimmers, L. Aigouy, M. Mortier, A. Sharoni, S. Wang, K. G. West, J. G. Ramirez, and I. K. Schuller, "Role of thermal heating on the voltage induced insulator-metal transition in VO2," Phys. Rev. Lett., vol. 110, p. 056601, 2013.

[16] P. Maffezzoni, L. Daniel, N. Shukla, S. Datta and A. Raychowdhury, "Modeling and simulation of vanadium dioxide relaxation oscillators," IEEE Trans. Circuits Syst. I, vol. 62, no. 9, pp. 2207–2215, Sept. 2015.

[17] C. Delacour and A. Todri-Sanial, "Mapping Hebbian Learning Rules to Coupling Resistances for Oscillatory Neural Networks", working paper or preprint, https://hal-lirmm.ccsd.cnrs.fr/lirmm-03197299, 2021.

[18] E. Corti, B. Gotsmann, K. Moselund, A. M. Ionescu, J. Robertson, and S. Karg, "Scaled resistively-coupled VO_2 oscillators for neuromorphic computing," Solid State Electron., vol. 168, 107729, 2020.

[19] E. Corti, J.A. Cornejo Jimenez, K. M. Niang, J. Robertson, K. E. Moselund, B. Gotsmann, A. M. Ionescu and S. Karg, "Coupled VO_2 Oscillators Circuit as Analog First Layer Filter in Convolutional Neural Networks", Frontiers in Neuroscience, vol. 15, 2021.

[20] R. Ge, X. Wu, M. Kim, J. Shi, S. Sonde, L. Tao, et al., "Atomristor: nonvolatile resistance switching in atomic sheets of transition metal dichalcogenides," Nano Lett., vol. 18, pp. 434–441, December 2017.

[21] M. Kim, R. Ge, X. Wu, X. Lan, J. Tice, J. C. Lee, et al., "Zero-static power radio-frequency switches based on MoS_2 atomristors," Nat. Commun., vol. 9, 2524, June 2018.

[22] J. Yoon, G. Lee, C. Park, B. S. Mun, and H. Ju, "Investigation of length-dependent characteristics of the voltage-induced metal-insulator transition in VO_2 film devices," Appl. Phys. Lett., vol. 105, 083503, 2014.

[23] L. Zhang, T. Gong, H. Wang, Z. Guo, and H. Zhang, "Memristive devices based on emerging two-dimensional materials beyond graphene," Nanoscale, vol. 11, pp. 12413–12435, 2019.

[24] E. Corti, B. Gotsmann, K. Moselund, I. Stolichnov, A. Ionescu and S. Karg, "Resistive coupled VO_2 oscillators for image recognition," 2018 IEEE International Conference on Rebooting Computing (ICRC), McLean, VA, U.S.A., pp. 1-7, 2018.

[25] "Edge tpu performance benchmarks," https://coral.ai/docs/edgetpu/benchmarks, accessed: 2020-04-06.

[26] T. Jackson, S. Pagliarini, and L. Pileggi, "An oscillatory neural network with programmable resistive synapses in 28 nm CMOS," 2018 IEEE International Conference on Rebooting Computing (ICRC), pp. 1–7, 2018.

[27] M. Abernot, T. Gil, M. Jiménez Juan Núñez, M. J. Avedillo, B. Linares-Barranco, T. Hardelin, T. Gonos, A. Todri-Sanial, "Digital Implementation of Oscillatory Neural Network for Image Recognition Application", working paper or preprint, https://hal-lirmm.ccsd.cnrs.fr/lirmm-03185020, 2021.